

# Through Wall Gap Detection Using Monostatic Radar

A. Elboushi<sup>1</sup>, A. R. Sebak<sup>1,2</sup>, and T. Denidni<sup>3</sup>

<sup>1</sup>Electrical and Computer Engineering Department,  
Concordia University 1455 de Maisonneuve West, EV005.127, Montreal, Quebec H3G 1M8, Canada  
ay\_moh@encs.concordia.ca

<sup>2</sup>KACST Technology Innovation Center in RFTONICS, KSU, Riyadh 11421, Kingdom of Saudi Arabia

<sup>3</sup>INRS Place Bonaventure, 900 De la Gauchetière Ouest, Niveau C, Montréal, Quebec H5A 1C6, Canada  
denidni@emt.inrs.ca

**Abstract** — In this paper, a new experimental system for through wall gap detection and concealed vacancies behind wall is introduced. The ultra wide band (UWB) system is based on the principles of time domain reflectometry (TDR) and ground-penetrating radar (GPR) for through wall imaging to detect hidden gaps and/or hiding persons behind walls. The system uses a very short pulse generated by the vector network analyzer (VNA) to illuminate the wall under investigation through an UWB antenna probe. The detection process is achieved using time domain measurements of the probe reflection coefficient  $S_{11}$ . Some numerical analyses have been carried out for verifying the principle of operation. The experimental results show a great ability not only for the gap detection between walls but also for estimation of the gap width with a very good accuracy (6.25 % in the worst case) for different types of walls.

**Index Terms** — GPR, monostatic radar, TDR, tunnels detection, time domain measurements, UWB antenna, and UWB pulse.

## I. INTRODUCTION

Recently, many research efforts have been exerted for developing modern microwave imaging systems to work in home land security and other applications. UWB technology has been used for some time in ground penetrating radar (GPR) applications [1-3] and early breast cancer detection [4-6]. Recently, as a new trend, it is used in through wall imaging applications to help police

to detect the existence of any hidden rooms or hidden people behind walls [7-9]. Many numerical analysis techniques have been employed for through wall imaging including geometrical optics (GO), ray tracing [10-11], and 2D method of moments (MoM) [12].

In this paper, a time domain reflectometry (TDR) UWB through wall gap detection system based on the operation principle of the UWB imaging system proposed by Chang et al [13] is presented. It is based on sending a short duration pulse that is synthesized by transmitting continuous wave (CW) signals at equidistant frequencies covering the entire UWB range from 3.1 GHz to 10.6 GHz. The signal is produced by a vector network analyzer (VNA) after proper calibration over the pre-stated frequency range. The time domain representation of the pulse can be obtained by performing inverse fast Fourier transform (IFFT) on both transmitted and received signals. The principle is used in [13] for building a complete UWB imaging system for breast cancer detection. Multiple numerical simulations have been carried out using a finite integration technique (FIT) simulator, CSTMWS [14], to address the possible multiple reflections due to the wall construction. These simulations are used to ensure the negligible effect of the higher order reflection on the gap detection accuracy.

The proposed UWB imaging system has an advantage over some of the available systems since it adopts the monostatic radar principle, i.e., it uses just one antenna for both transmission and reception. The UWB sensor is also another critical

design parameter regarding the cost, weight, and size. In the proposed system the heavy metallic UWB horn sensor is replaced by a low profile UWB microstrip antenna to maintain a high accuracy detection level.

## II. THE PROPOSED THROUGH WALL GAP DETECTION SYSTEM

The proposed UWB imaging system for through wall gap detection is shown in Fig. 1. The system includes a fixed support to mount an UWB probe antenna. The probe antenna is connected to channel (1) of the VNA. An absorber is mounted vertically behind the antenna to prevent any undesired back reflections. The antenna is centered to face the first wall in the  $y$ - $z$  plane, whereas the separation distance between the antenna and the first wall should be chosen carefully to ensure working in the far-field region of the antenna. Undesired reflections in UWB imaging systems considered as a great obstacle. To overcome this problem we focus on a prototype, which images the target using a synthesized pulse realized by sending continuous signals at equidistant frequencies over the required microwave band [13]. In order to check the imaging system capabilities for detecting hidden gaps behind walls, we made some practical tests using the setup shown in Fig. 1. The proper choice of the UWB antenna sensor is very critical issue for the system. In [15] three different UWB antenna prototypes were presented and maybe used as antenna probes covering the frequency band from 3 GHz to 10 GHz. The first prototype, shown in Fig. 2, consists of an elliptical aperture etched out from the ground plane of a PCB and a microstrip line with half circular shaped ring stub for excitation, which is chosen to work as an antenna probe in this system to satisfy the impedance bandwidth of the UWB range, as shown in Fig. 3, it relatively has a constant gain and stable radiation patterns over the UWB frequency range. The optimized antenna parameters in [15] are chosen according to multiple parametrical studies and optimizations carried out using CSTMWS. The final design antenna parameters are shown in Table 1.

Two different wall materials were studied. The first type with thickness equal 3 cm, length equals to 22 cm, and width equal to 30 cm is made of a reinforced papers with a lower attenuation

coefficient (0.26 dB/cm) than the second one. The second material (5.5 cm thickness, 23 cm length, and 15 cm width) is made of sandy brick and has a very high attenuation coefficient (3.6 dB/cm). Figures 4 and 5 show different reflections from two walls separated by an air gap and from a solid wall, respectively. As shown in Fig. 3, we expect four reflection coefficients ( $\Gamma_1, \dots, \Gamma_4$ ) in case of having a gap between the two walls.

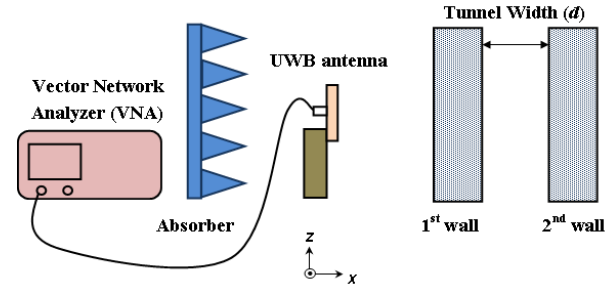


Fig. 1. The proposed UWB imaging system for through wall gap detection.

Table 1: Optimized dimensions for the UWB antenna (in mm) [15].

Parameter	Value
W	45
L	45
$W_1$	3
$L_1$	12.4
S	1.4
$R_1$	4.5
$R_2$	11
A	9.6
B	19

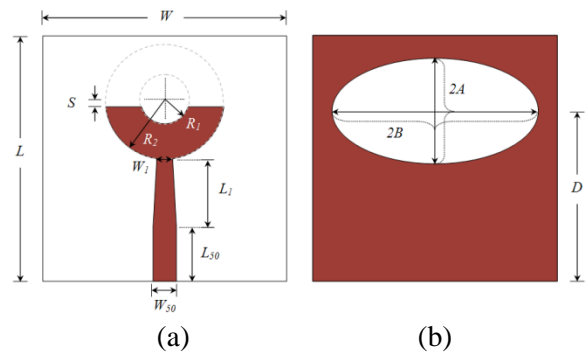


Fig. 2. Geometry of the UWB antenna [15] (a) front view and (b) back view.

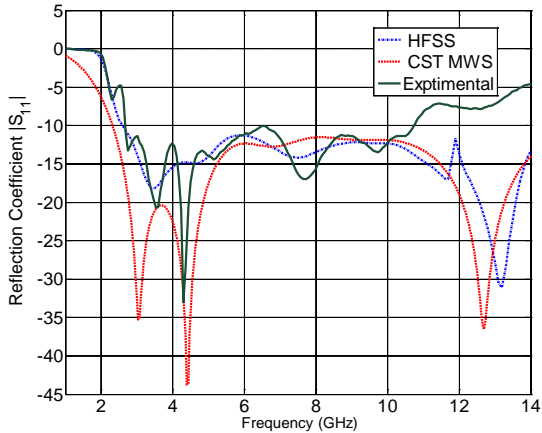


Fig. 3. Simulated and experimental return loss  $S_{11}$  of the UWB antenna [15].

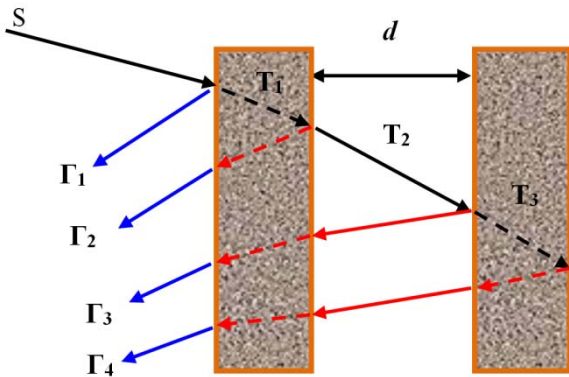


Fig. 4. Reflections from the 1<sup>st</sup> and the 2<sup>nd</sup> wall with a gap in between.

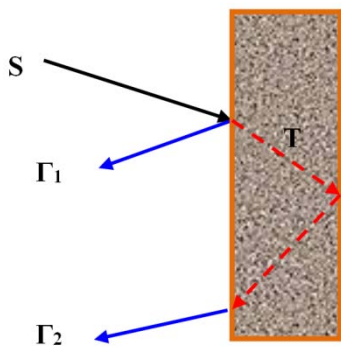


Fig. 5. Reflections from a solid wall without gaps.

The gap detection algorithm begins by reading the reflection coefficient ( $S_{11}$ ) from the VNA to obtain a frequency domain representation for the wall(s) reflections  $G(f)$ . Using inverse fast Fourier

transform (IFFT) embedded code in the VNA, a time domain representation of the reflection can be obtained  $g(t)$ . In order to cancel the antenna, cables and connectors effect, the received reflections  $g(t)$  are subtracted from the antenna response in front of an absorber  $a(t)$ . The resulted signal  $s(t)$  contains only the reflection information from the wall(s) under study. By monitoring the peaks and their locations, the detection algorithm will provide enough information to make a decision in regard to the structure with either a solid wall or two walls separated by a gap ( $d$ ). The gap ‘tunnel’ width ( $d$ ) separating the two walls can be evaluated using the separation time ( $t$ ) between the second reflection  $\Gamma_2$  and the third reflection  $\Gamma_3$  from the following equation,

$$d = (t * c)/2 \tag{1}$$

where  $c$  is the speed of light in free space. The flow chart of the gap detection algorithm is shown in Fig. 6.

### III. NUMERICAL INVESTIGATION OF THROUGH WALL GAP DETECTION USING CSTMWS

In order to verify the proposed system performance and study the possible sources of errors, especially from higher order reflections, some numerical simulations have been carried out using CSTMWS [14] simulator. Two different cases have been investigated to determine the expected time domain reflections. The first one is the single wall, while the second is two walls separated by an air gap ( $d$ ). An UWB plane wave Gaussian pulse (3 GHz to 10 GHz), shown in Fig. 7, is used as a source of an incident wave, while the reflected back signals are monitored on the surface of the first wall. Two different scenarios for the internal construction of the walls under study are assumed. The first is for a lossless case with zero conductivity as an extreme case with no attenuation. While the other one assumes an actual sandy brick walls with finite conductivity ( $\epsilon_r = 5.84$  and the conductivity  $\delta = 89$  mS/m).

Figure 8 shows a comparison between the time domain reflection from the single wall and the reflections of the two walls separated by an air gap of 5 cm assuming the worst case of lossless walls with zero conductivity. It can be concluded that the first and second reflections for both cases are coincident with each other. However, the multiple

reflections (i.e., higher order reflections inside the single wall) are responsible for the lower amplitude reflections around 2.3 ns (solid red curve). The amplitudes of these reflections are much smaller compared with  $\Gamma_3$ . Figure 9 shows the reflections according to the second scenario of using sandy bricks walls. The effect of the higher order reflections decreased dramatically so that it cannot interfere with  $\Gamma_3$ . In the case of the two walls reflections, the air gap separation ( $d$ ) is responsible for the time difference between  $\Gamma_2$  and  $\Gamma_3$ . Some parametrical studies for different values of ( $d$ ), shown in Fig. 10, illustrate that effect.

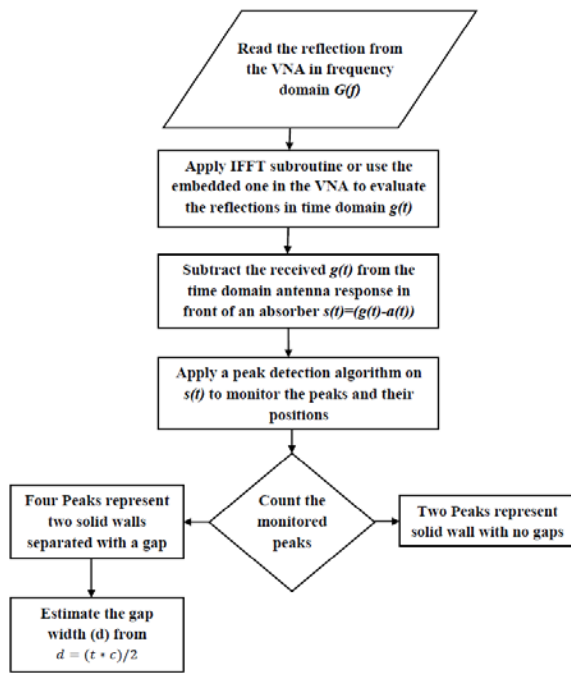


Fig. 6. Gap detection algorithm.

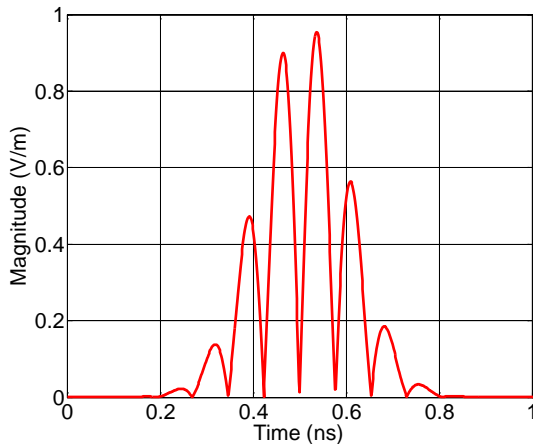


Fig. 7. UWB plane wave pulse used by CSTMWS.

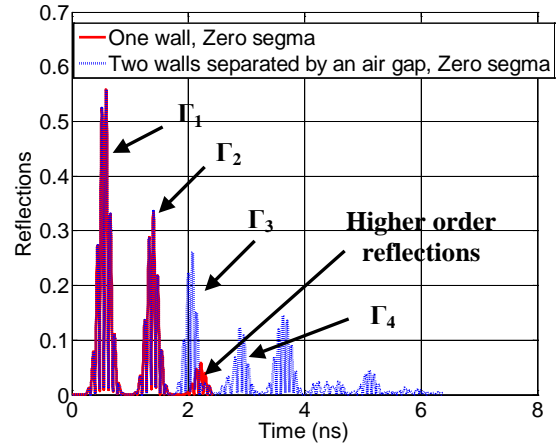


Fig. 8. Time domain reflection comparison using no attenuation walls.

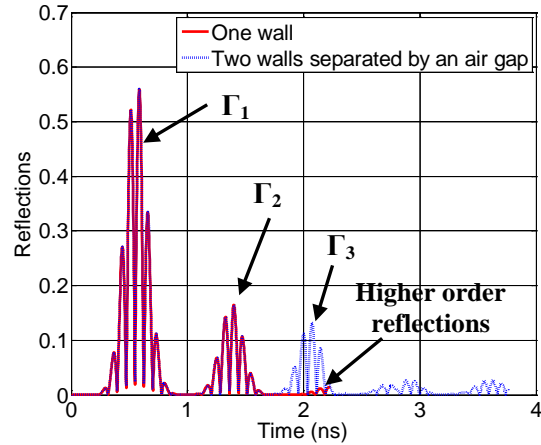


Fig. 9. Time domain reflection comparison using sandy bricks walls.

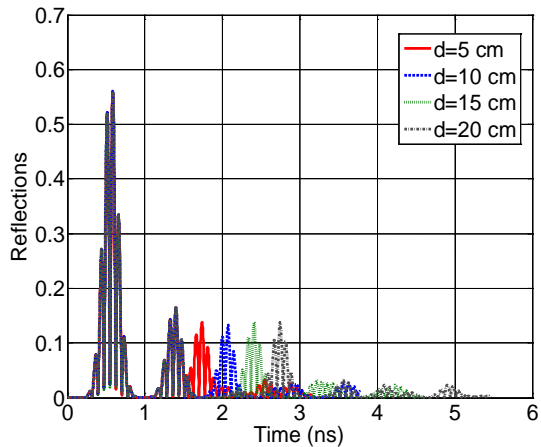


Fig. 10. Time domain reflections of two walls for different values of the air gap separation ( $d$ ).

### A. 1D Time domain results using one wall

After constructing the system shown in Fig. 1 and calibrating the VNA using standard calibration procedure in the frequency range of 3 GHz to 10 GHz, we measure the reflection coefficient in the frequency domain and then using the time domain conversion tool embedded in the VNA, we convert the response into time domain. Figure 11 shows the antenna response in front of an absorber and without any walls, where we can notice two large reflection peaks and some small reflections at a later time. The first peak accounts for the reflection from the interface between the microstrip feed line and the antenna, while the second peak results from reflection of the electromagnetic wave radiated by the antenna into free space. The minor reflections at later time can be accounted to multipath effects and scattering waves from the surrounding objects. Figure 12 shows a comparison between the time domain antenna response in front of an absorber and the response in front of a single low attenuation wall, 19 cm apart, where two huge peaks appeared as a result of the air/wall reflection ( $\Gamma_1$ ) and wall/air reflection ( $\Gamma_2$ ). Figure 13 (a) and 13 (b) shows a photo for the measurement setup.

### B. 1D Time domain results using two walls of low attenuation coefficient with a gap between them

Figure 14 (a) to 14 (e) shows the multiple reflections due to two walls separated by a distance  $d$ . Table 2 shows a comparison between the actual gap dimensions and the calculated ones using equation (1). There is a good agreement between the actual and the calculated separation  $d$ , where the percentage error does not exceed 6.25 % for the considered cases. The error pattern here does not follow a certain pattern because of errors in antenna location adjustment, minor errors in the actual distance measurements and some errors due to multipath effect from the surrounding objects.

### C. 1D Time domain results using two walls of high attenuation coefficient with a gap between them

The nature of the wall material has a great effect on the reflected back signals from the walls, for example, using a high attenuation walls (sandy bricks) will results in much lower reflection levels ( $\Gamma_2$ ,  $\Gamma_3$ ,  $\Gamma_4$ ) after the first reflection. Time domain

representation is shown in Fig. 15 for the reflections occur from a solid wall in front of the transreceiving antenna. The distance from the antenna probe to the first wall is reduced to 10 cm for reducing the round trip path loss. Two major peaks can be noticed; the first one is due to the air/wall reflection and the second is due to the wall/air reflection whose magnitude is very low (less than -60 dB) mainly due to the wave high attenuation inside the wall. Figure 16 illustrates the effect of 5.5 cm gap between the two walls, where just three reflections ( $\Gamma_1$ ,  $\Gamma_2$ ,  $\Gamma_3$ ) can be detected while the fourth one ( $\Gamma_4$ ) cannot be detected because of the interference with the noise floor due to its small value. The calculated distance between the two walls is 5.25 cm, which is compared to the actual distance (5.5 cm) with a percentage error of 4.54 %.

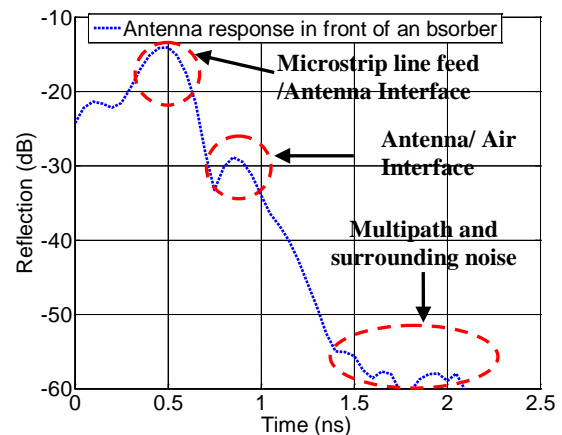


Fig. 11. Antenna response in front of an absorber.

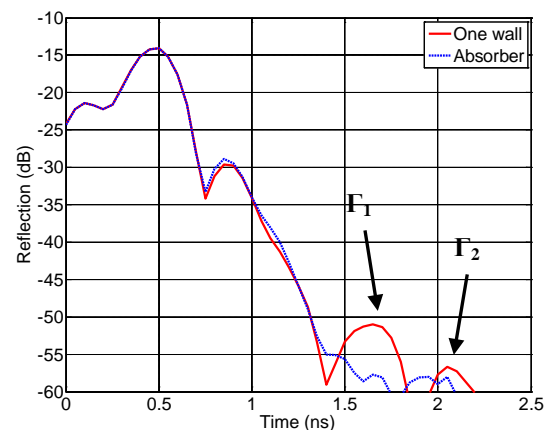


Fig. 12. Reflections from a solid low attenuation wall without gaps.

Table 2: Comparison between the actual and the calculated gap length between walls.

Actual Distance between two walls	Calculated Distance between two walls	Error %
7 cm	6.75 cm	3.5 %
8 cm	7.5 cm	6.25 %
10 cm	9.75 cm	2.5 %
12 cm	11.25 cm	6.25 %
15 cm	15 cm	0 %



(a)



(b)

Fig. 13. Practical measurement arrangements (a) solid sandy brick wall and (b) two walls separated by a distance  $d$ .

#### IV. CONCLUSION

In this work, an accurate and easy to built UWB through wall gap detection system based on TDR approach is presented. Some numerical and practical UWB imaging experiments have been carried out for gap detection between walls made of different materials using time domain measurements. The proposed system shows a remarkable performance in both gap detection and gap width determination with a very high precision with an error percentage not more than 6.25 % in the worst case.

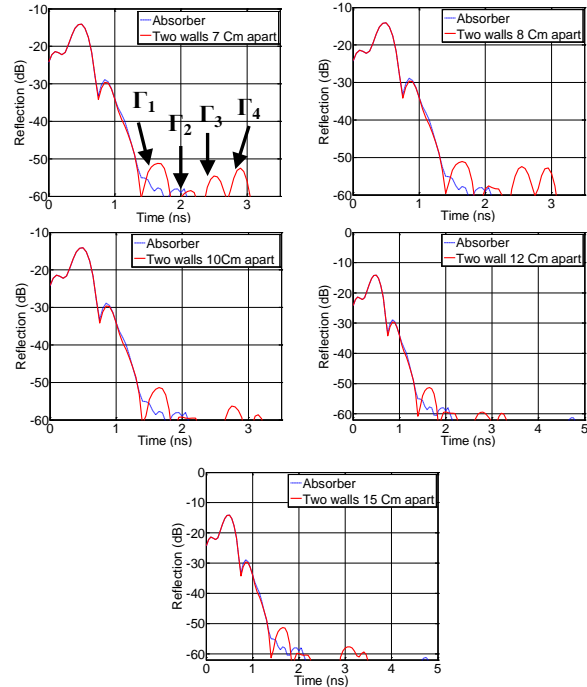


Fig. 14. Reflections from two low attenuation walls separated by an air gap (d).

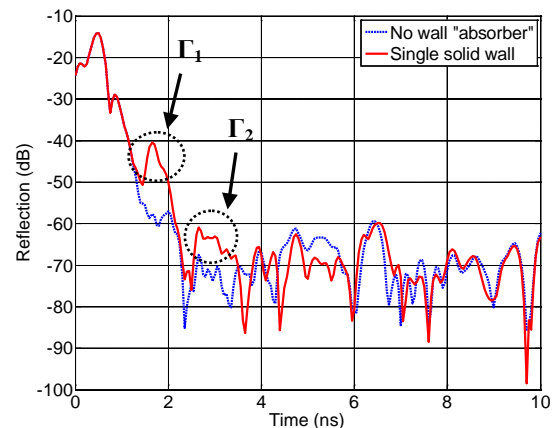


Fig. 15. Reflections from a solid single high attenuation wall without gaps.

#### ACKNOWLEDGMENT

This work is partly funded by the Canadian NSERC Discovery Program. And by a grant from King Abdulaziz City of Science and Technology (KACST)-Technology Innovation Center in RFTONICS at King Saud University.

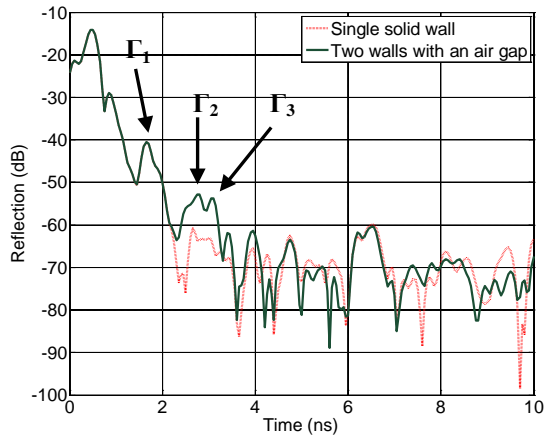


Fig. 16. Reflections from two high attenuation walls separated by an air gap of 5.5 cm.

### REFERENCES

- [1] A. B. Suksmono, E. Bharata, A. A. Lestari, A. G. Yarovoy, and L. P. Ligthart, "Compressive stepped-frequency continuous-wave ground-penetrating radar," *IEEE Geoscience and Remote Sensing Letters*, vol. 7, no. 4, pp. 665-669, Oct. 2010.
- [2] C. -L. Huang, S. -P. Zhu, and M. Lu, "Miniature multimode deep ground penetrating radar," *13<sup>th</sup> International Conference on Ground Penetrating Radar (GPR)*, pp. 1-5, 21-25 June 2010.
- [3] Y. Sun and J. Li, "Time-frequency analysis for plastic landmine detection via forward-looking ground penetrating radar," *IEE Proceedings on Radar, Sonar, and Navigation*, vol. 150, no. 4, pp. 253-261, Aug. 2003.
- [4] Y. Zhou, "Microwave imaging based on wideband range profiles," *Progress In Electromagnetics Research Letters*, vol. 19, pp. 57-65, 2010.
- [5] R. C. Conceição, M. O'Halloran, M. Glavin, and E. Jones, "Comparison of planar and circular antenna configurations for breast cancer detection using microwave imaging," *Progress In Electromagnetics Research*, vol. 99, pp. 1-20, 2009.
- [6] S. A. AlShehri and S. Khatun, "UWB imaging for breast cancer detection using neural network," *Progress In Electromagnetics Research C*, vol. 7, pp. 79-93, 2009.
- [7] F. Aryanfar and K. Sarabandi, "Through wall imaging at microwave frequencies using space-time focusing," *IEEE Antennas and Propagation Society International Symposium*, vol. 3, pp. 3063-3066, 20-25 June 2004.
- [8] K. M. Yemelyanov, N. Engheta, A. Hoorfar, and J. A. McVay, "Adaptive polarization contrast

techniques for through-wall microwave imaging applications," *IEEE Transactions on Geoscience and Remote Sensing*, vol. 47, no. 5, pp. 1362-1374, May 2009.

- [9] V. M. Lubecke, O. Boric-Lubecke, A. Host-Madson, and A. E. Fathy, "Through-the-wall radar life detection and monitoring," *IEEE Microwave Symposium*, pp. 769-772, June 2007.
- [10] C. Thajudeen, W. Zhang, and A. Hoorfar, "Efficient forward modeling of large scale buildings and through-the-wall radar imaging scenarios," *28<sup>th</sup> Annual Review of Progress in Applied Computational Electromagnetics (ACES)*, Columbus, Ohio, pp. 122-126, April 2012.
- [11] A. Buonanno, M. D'Urso, G. Prisco, M. Ascione, and A. Farina, "A model-based signal processor to see inside buildings," *26<sup>th</sup> Annual Review of Progress in Applied Computational Electromagnetics (ACES)*, Tampere, Finland, pp. 846-851, April 2010.
- [12] A. Buonanno, M. D'Urso, G. Prisco, M. Ascione, and A. Farina, "A model-based signal processor to see inside buildings," *26<sup>th</sup> Annual Review of Progress in Applied Computational Electromagnetics (ACES)*, Tampere, Finland, pp. 846-851, April 2010.
- [13] K. W. Chang, M. E. Bialkowski, and S. Crozier, "Microwave imaging using a planar scanning system with step-frequency synthesized pulse," *Asia-Pacific Conference Proceedings on Microwave*, APMC, vol. 1, pp. 4, 4-7 Dec. 2005.
- [14] CST Microwave Studio, ver. 2012, Framingham, MA, 2012.
- [15] A. Elboushi, O. M. H. Ahmed, A. R. Sebak, and T. A. Denidni, "Study of elliptical slot UWB antennas with a 5.0-6.0 GHz band-notch capability," *Progress In Electromagnetics Research C*, vol. 16, pp. 207-222, 2010.



**Ayman Elboushi** was born in Zagazig, Egypt, in 1978. He received the B.Sc. degree in Electrical Engineering from Zagazig University, Zagazig, Egypt, in 2000, and M.Sc. degree in Electrical Engineering from Ain Shams University, Cairo, Egypt, in 2007.

From 2001 till 2008, he worked as a researcher assistant in Electronics Research Institute (ERI), Microstrip Dept., Cairo, Egypt. In 2008, he joined the Microwave group of Department of Electrical and Computer Engineering, Concordia University, as a researcher assistant and he is now working towards his Ph.D. degree.



**Abdel-Razik Sebak** received the B.Sc. degree in Electrical Engineering from Cairo University in 1976 and the M. Eng. and Ph. D. degrees from the University of Manitoba in 1982 and 1984, respectively. From 1984 to 1986, he was with the Canadian Marconi Company. From 1987 to 2002, he was a Professor of Electrical and Computer Engineering, University of Manitoba. He is currently a Professor of Electrical and Computer Engineering, Concordia University. His current research interests include phased array antennas, computational electromagnetics (EM), integrated antennas, EM theory, interaction of EM waves with new materials, and bio-EM. Dr. Sebak received the 2000 and 1992 University of Manitoba Merit Award for outstanding Teaching and Research, the 1994 Rh Award for Outstanding Contributions to Scholarship and Research in the Applied Sciences category, and the 1996 Faculty of Engineering Superior Academic Performance. He has served as Chair for the IEEE Canada Awards and Recognition Committee (2002–2004).



**Tayeb A. Denidni** received the B.Sc. degree in Electronics Engineering from the University of Setif, Setif, Algeria, in 1986, and the M.Sc. and Ph.D. degrees in Electrical Engineering from Laval University, Quebec, Canada, in 1990 and 1994, respectively. From 1994 to 2000, he was a Professor with the Engineering Department, Université du Québec, Rimouski, Quebec, Canada. Since August 2000, he has been a Professor with Institut National de la Recherche Scientifique (INRS), Université du Québec, Montreal, Canada. He is leading a large research group consisting of two research scientists, five Ph.D. students, and three M.Sc. students. Over the past 10 years, he has graduated numerous graduate students. His current research interests include planar microstrip filters, dielectric resonator antennas, EM-bandgap antennas, antenna arrays, and microwave and RF design for wireless applications. He has authored over 110 papers in refereed journals. He has also authored or coauthored over 150 conference papers.